EAI Endorsed Transactions
on Scalable Information Systems
Research Article EAI.EU

A Microservices-based Framework for Real-time Carbon Emission Monitoring and Visualization of Large-scale Building Clusters

Raoying Lv[1*], Cheng Zhu[2]

[1]School of Civil Engineering Architecture, Zhejiang Guangsha Vocational and Technical University of Construction, Dongyang, Zhejiang, China
[2]College of Architectural Engineeing, Jiaxing Nanhu University, Jiaxing, Zhejiang, China

Abstract

Although being one of the largest operational CO_2 contributors, current monitoring systems rely largely either on top-down inventories or sparse bottom-up sensor measurements, leading to coarse temporal visibility and reduced real-time responsiveness. Classic methods, like ARIMA and basic rule-based aggregation, cannot handle nonlinear variations, high-frequency fluctuations and cross-domain inconsistency; hence, their suitability is considerably limited for city-scale tracking of building cluster emissions. This paper attempts to fill some of the gaps by proposing a microservices-based real-time carbon emission monitoring and visualization framework, which fuses heterogeneous macro-scale CityGHG inventories with micro-scale UCI smart-meter datasets. It discusses data collection from the sectoral CO_2 records of CityGHG in 2015-2020 and high-resolution streams of household energy consumption from the UCI repository. After preprocessing, emissions were normalized using sector-specific emission factors and converted into fine-grained CO_2eq series. Subsequently, an LSTM-based forecasting module was employed due to its superiority in modeling nonlinear seasonality and long-term dependencies. Strong performance in forecasting was recorded, with Proposed returning the minimum MAE, MAPE, and RMSE as 0.0269, 0.3644, and 0.0113, respectively, and ARIMA and MLP results being moderate at 0.0898 and 0.0395 for MAE and 0.4150 and 0.7241 for MAPE, respectively. Cross-domain validation revealed distributional consistency across cities by showing an overall KL divergence of 0.0561, while DTW distances of 2.78 to 4.38M reflected temporal similarity between micro-domain and macro-domain sequences. Proposed framework has scalable real-time estimation, increased interpretability and multi-resolution visualization of results as required for operational decision-making. Altogether, this work proposes a deployable, auditable and adaptable architecture for the next generation of carbon monitoring over large-scale building clusters.

Keywords: Real-time carbon monitoring, Microservices architecture, CO_2-equivalent forecasting, CityGHG, Building clusters

Received on 20 November 2025, accepted on 31 August 2026, published on 26 November 2026

Copyright © 2026 Raoying Lv *et al.*, licensed to EAI. This is an open access article distributed under the terms of the CC BY-NC-SA 4.0, which permits copying, redistributing, remixing, transformation, and building upon the material in any medium so long as the original work is properly cited.

doi: 10.4108/eetsis.10994

*Corresponding author. Email: lvraoying@126.com

1. Introduction

Urban buildings constitute one of the significant sources of operational greenhouse-gas emissions and extensive aggregation of buildings generates considerable spatiotemporal variation of energy consumption and CO_2 emissions [1]. The accelerated urbanization and decarbonization is not only in China but also across other

regions of the world has enhanced the need to have monitoring instruments that offer high resolution and auditable emission estimates in a city-district scale [2]. Precise, nontemporal visibility of cluster emissions of buildings can be used to make operational decisions, demand response and policy check at municipal levels [3]. Both top-down benchmarking and bottom-up operational control of the building can be assisted by combining historical city-level baselines with building-level telemetry. National and city datasets are several recent datasets that have enhanced the baseline accounting and offer the historical context of the training and validation of the models. With these datasets, long-term inventories can be combined with real-time data of smart meters to create actionable insights [4]. Real time monitoring frameworks therefore fills the loopholes in the management of energy, emissions accounting and policy compliance to the stakeholders of urban areas.

Other previous studies have applied rule-based and statistical aggregation pipelines to predict building emissions using energy meters; both are easy to interpret and simple to use, but may not always observe time effects or non-linear behavior across heterogeneous clusters [5]. ARIMA (Auto Regressive Integrated Moving Average) and Proposed are time-series forecasting techniques that have been used to predict demand and emissions, but they have difficulties in non-stationary patterns, multi-scale seasonality, and cross-building interactions [6]. Machine-learning regressors (e.g., XGBoost, SVR) run under supervision create good short-term predictions with good feature availability but with large amounts of labelled data and also tend to be unresponsible to the sequence structure of time [7]. Wholly model-based energy simulation models offer physical interpretability at a high cost to be able to calibrate with large populations of heterogeneous buildings [8]. These constraints decrease the strength in detection of anomalies, lower the prediction precision in case of extreme events and make the system difficult to apply in large scale.

Recently LSTM (Long Short-Term Memory) networks and sequence autoencoders have been applied to learn temporal dependencies and identify anomalous consumption patterns with superior results on non-linear and multi-scale time series [9]. Unsupervised approaches such as Tree-based Isolation Forest and ensemble detectors are small and apply to sparse anomalies, but do not have a temporal context and tend to falsely reject seasonally changing loads [10]. Hybrid systems that integrate physics-based models with data-driven modules are a partial solution that makes interpretability more complex and costly to integrate [11]. Numerous previous systems also have no provenance of emission factor or scaleable microservices architecture making scalable real-time operation on large clusters hard. These loopholes drive a structure that is interpretable, scalable and predictable [12].

While large-scale emission inventories and high-frequency sensor data are increasingly available, there is still a lack of an integrated architecture in current systems that can synergize heterogeneous sources to support real-time city-to-household carbon monitoring. Current models are either at the macro level for historical forecasting or at the micro level for power analytics and barely support cross-domain calibration, dynamic scaling, or continuous online processing. To address this challenge, this study designs a framework for real-time carbon emission monitoring and visualization based on microservices across large-scale building clusters. It decouples data ingestion, preprocessing, emission factor normalization, forecasting and validation into modular microservices, ensuring flexibility, scalability and cross-domain interoperability. Therefore, this architecture allows seamlessly linking historical CityGHG emissions with real-time UCI smart meter data, from which a solid basis of multi-resolution CO_2eq estimation, automated forecasting, and dynamic visualization is enabled. The proposed system further enhances urban energy-emission intelligence by offering a deployable service-oriented solution that overcomes traditional limitations from monolithic analytic pipelines. The novelty of the proposed framework is the combination of macro-scale CityGHG inventories and micro-scale UCI smart-meter streams through a microservices-based architecture for real-time CO_2eq monitoring. Related work on real-time carbon monitoring system is mainly concentrated on analyzing city level inventories and monitoring energy in a single household, without relating these two domains. Instead, and present a macro-to-micro emission mapping process that converts city-level carbon signatures to household-level CO_2eq within the proposed framework. The suggested approach also performs structural cross-domain validation based on the Kullback-Leibler divergence and the Dynamic Time Warping (DTW) unlike previous LSTM based emission forecasting methods, which mainly concentrate on prediction accuracy only. The architecture also separates ingestion, preprocessing, forecasting, validation, and visualization into independently scalable services for deployment flexibility. These contributions, when taken together, clearly differentiate the proposed approach from traditional monolithic monitoring and single-domain prediction methods.

Contributions:

- Design a microservice-oriented city-scale carbon monitoring framework by seamlessly integrating heterogeneous macro-scale CityGHG with micro-scale UCI smart meter datasets that will help in real-time yet scalable estimation of CO_2eq across building clusters.
- Design a single emission factor normalization pipeline that projects historical, city-level CO_2 signatures onto household-level electricity streams by making use of sector-specific EF computation, cross-domain energy equivalence and temporal alignment equations.
- Implement, using LSTM architectures, a sequence forecasting model that can learn long-term nonlinear emission evolution from the CityGHG datasets and project the learned macro emission patterns into the

micro domain for predictive estimation of CO_2eq behaviour.
- Validate the cross-domain robustness of the proposed framework using dual evaluation metrics, namely forecast accuracy metrics (RMSE, MAE, MAPE, R^2) and structural alignment measures ((KL Divergence (Kullback–Leibler Divergence), DTW (Dynamic Time Warping) to demonstrate improved transferability and emission consistency across scales.

1.1 Problem Statement

ARIMA models assumed stationarity, and their mechanisms were based on fixed seasonal patterns, thus being inappropriate for capturing abrupt regime changes in urban energy demand [13]. They were susceptible to noise and missing values that are common in large IoT streams and resulted in biased short-term estimates of CO_2-eq. Their univariate nature usually neglected cross-building correlations and spatial heterogeneity within city clusters. In fact, these methods did not work well if applied alone for real-time emission monitoring and operational alerts.

Proposed-style models captured the broad trends and seasonality but failed to be responsive in a fine-grained manner to sub-hourly events in building clusters. They were not natively set up for multisource streaming inputs and were at a disadvantage under high-frequency IoT noise [14]. Forecasting uncertainty estimates often did not reflect rapid grid-mix emission-factor changes and hence reduce auditability. Therefore, relying on these methods alone undermines timely anomaly detection and informed decision support for cluster-level emissions.

Isolation Forest and other point detectors flagged outliers but did not have temporal context, leading to false positives on seasonal or occupant-driven variations. CNN-based spatial hybrids necessarily require dense spatial grids or image-like inputs, often not available for heterogeneous building clusters [15]. Both families also struggled to provide traceable causes or provenance for the flagged emission events, impeding audit and policy reporting. Therefore, they are not good enough as stand-alone detectors of auditable, operational monitoring of emissions across large urban clusters.

1.2 Research Objective

- Analyze the heterogeneous macro-scale and micro-scale data of CityGHG and UCI smart meters for developing a unified modeling framework of carbon emissions.
- Derive sector-specific emission factors from historical CityGHG records for normalizing high-frequency micro-domain electricity consumption signals.
- Design a conversion pipeline for CO_2eq that converts smart-meter real-time energy streams into a micro-domain emission series based on an EF-based mapping.
- Design a sequence-learning model (LSTM-based) that captures long-term temporal patterns, seasonality and nonlinear emission dynamics.
- Assess forecasting performance using standard accuracy metrics: RMSE, MAE, MAPE, R^2. Check the compatibility across domains using KL Divergence and DTW.

1.3 Structure of Paper

Paper is organized as follows: Section 1 introduces the background and motivation of real-time carbon monitoring in large building clusters. Section 2 reviews related literature on microservices, emission datasets, forecasting models and visualization approaches. Section 3 elaborates on the proposed methodology including data collection, preprocessing, computing the emission factor, constructing micro-domains of CO_2eq, LSTM forecasting, and cross-domain validation. Section 4 presents experimental results and discussion, including weekly emission patterns, forecasting performance by using RMSE, MAE, MAPE, R^2 and structural similarity analyses including KL and DTW. Section 5 concludes the study by discussing the limitations and future research directions.

2. Literature Survey

2.1 Microservices & Real-Time Systems

El Akhdar et al. [16] investigated the advantages of microservices in IoT systems regarding scalability, fault-isolation and rapid deployment of service components. They compared microservices with monolithic architectures and argued that microservice designs are far more flexible for large device networks. This also helped inform service-based ingestion and processing layers in real-time frameworks. To manage energy in smart homes and buildings, their study focused on the best practices for using microservices rather than sensor-rich systems.

Ortiz et al. [17] provided versatile microservice architecture with high efficiency and modularity. They applied this architecture to industrial sensor networks and showed improvements in throughput and maintainability. Their framework demonstrated how service granularity enables dynamic scaling in streaming contexts. Findings support designing ingestion and stream-processing microservices in emission monitoring systems.

Nuñez-Skowronek et al. [18] developed a microservices-based architecture that mainly depends on modular service layers and REST-API-driven communication. They addressed service orchestration and building system heterogeneity for controllability and efficiency. The results presented show that real-time carbon emission monitoring requires microservice design to balance granularity with performance overhead. This work should inform such decisions on service design in scalable frameworks.

Gheorghe [19] reviews the novel generations of IoT reference architectures and highlight the importance of scalable, modular and cloud–edge–fog integrated system architecture directly supporting microservices-based real-time monitoring frameworks for large-scale distributed applications (e.g., monitoring carbon emissions in building ensembles).

2.2 Emission Data & Building Clusters

Ratra et al. [20] introduced an energy-aware microservices architecture for massive distributed platforms and illustrated modular service orchestration along with scalable resource management to enhance the efficiency of operation and real-time processing, which is closely applicable for monitoring carbon emissions over large-scale building packings. The city-level data with granularity enables the calibration of emission-factor components in monitoring systems. Their study directly relates to large-scale building cluster monitoring within China.

Wang et al. [21] developed a city-scale, gridded inventory of CO_2 emissions in Chengdu by disaggregating sectoral emissions to a 1 km grid using open data and proxies. This provides high-resolution spatial distribution of emissions that allows mapping high-emission zones. Such spatial data underpins visualization and cluster aggregation in frameworks for emission monitoring. In addition, this method enhances the geospatial component of building-cluster emission monitoring.

Kaginalkar et al. [22] planned SmartAirQ, a big-data governance framework for urban environments applying service-oriented architecture to air-quality monitoring, data acquisition, communication, processing and visualization. Although their domain is air quality, the service layers and data flows reflect what will be required in carbon emission monitoring within building clusters. The framework of Kaginalkar et al. demonstrates how multi-plane services can support urban environmental monitoring at scale. It provides good architecture references for emissions monitoring in cities.

Popović et al. [23] introduced a fog-based infrastructure for large-scale sensing of low-cost air quality sensors, encapsulating sensor-side microservices, edge/fog tiers, and cloud collaboration. Although focused on air quality, the tiered architecture and microservice encapsulation map well into real-time building emissions monitoring with IoT meters. Their system emphasizes sensor lifecycle, edge buffering and hierarchical architecture relevant to large-scale building clusters.

2.3 Forecasting Models

Araújo et al. [24] performed a review of the literature on energy consumption in microservices architectures and pointed out that service decomposition, distributed communication, and orchestration techniques have a strong impact on scalability, computational efficiency, and operational sustainability in big data real-time systems. Their results highlight the need for energy-aware microservice design for scalable carbon emission monitoring and visualization frameworks for heterogeneous building ensembles.

Xiong [25] developed a hybrid model of iForest-AE for energy anomaly detection in high-dimensional sensor data. Isolation Forest-based approaches generally enable detection of point anomalies, i.e., single data instances that deviate significantly from the whole dataset's statistical distribution. These represent false positives due to abrupt operational disturbances, or sensor faults and communication errors. Real-world building energy systems, however, also have contextual anomalies which are data points that are statistically normal when viewed in isolation, but are abnormal in a certain temporal or environmental context. For instance, high energy use during unoccupied time and unexpected night-time load patterns might be contextual anomalies although they are well within the expected numerical ranges. Temporal resolution and contextual dependency modeling are unavailable in Isolation Forest, and it is therefore not straightforward to interpret such dynamic behaviors as legitimate seasonal or occupant-induced variations. Thus, the approach may mistake the regular periodic consumption for anomalous ones and thus increasing the false-positive detection in the environment of multi-buildings monitoring. This is impeding the accuracy of isolation Forest based method for dynamic real-time CO_2eq monitoring. They showed that prefilters with iForest enhanced the performance of autoencoders when training data is polluted by latent anomalies. Their findings provide clues toward robust design of anomaly detection in the monitoring of building-cluster emissions.

Nayak et al. [26] introduced deep learning architecture using Transformer for energy consumption time series forecasting across multiple sites. Their multi-site forecasting architecture is relevant to predicting next-day emissions in building-clusters frameworks that aggregate many sensors. This supports scalability of predictive modules.

Feng et al. [27] discovered that ensemble techniques frequently performed better than single models given non-stationary data. Their comparison analysis supports the choice of cutting-edge forecasting models in emission-monitoring frameworks such as LSTM/GRU. Their results highlight the necessity of nonlinear models for real-time monitoring

2.4 Visualization & Decision Support

Alharkan et al. [28] anticipated a dual-stream CNN-LSTM model for solar/energy prediction and integrated attention mechanisms for feature importance, whose visualization of multi-site sensor results supported dashboard design. While the application to which they had devoted their work focused on solar forecasting, the hybrid model and insights into visualization apply to building-cluster emission

dashboards when combining spatial and temporal data. In this context, their work will inform dashboard design for real-time monitoring frameworks.

Pan et al. [29] applied Bayesian-optimized XGBoost to the life-cycle carbon prediction proxies with feature-driven explainability and dashboard-ready output. Their integration of explainable ML with visualization will support decision-making for facility managers and policymakers. Their study indicates how monitoring results can feed actionable dashboards within carbon emission frameworks for building clusters.

3. Methodology

Proposed framework combines macro-level historical emissions data with high-frequency household electrical consumption streams to build a unified CO_2-equivalent forecasting architecture as shown in Figure 1. Overall, methodological workflow is structured into six key layers as illustrated in the system architecture. Each layer transforms and transfers information across domains, city-scale (macro) and smart-meter (micro) by progressively refining emission factors, temporal patterns and cross-domain consistency. The proposed framework is based on a distributed microservices architecture, where each functional block is realized as an individual service, to enhance scalability, modularity, fault isolation and real-time responsiveness. The architecture has six core services: data ingestion, preprocessing, CO_2eq transformation, LSTM forecasting, validation, and visualization. The data ingestion agent perpetually collects cityGHG inventory data and UCI smart-meter data from heterogeneous sources via RESTful APIs and HTTP-enabled transport protocols at an average rate of 2.3 MB/s. The data packets received are then made to move along asynchronous processing pipelines, wherein a set of preprocessing services apply temporal synchronization, interpolation, normalization, and outlier removal to raw data sequences for input to the CO_2eq transformation layer. The resulting transformed emission sequences are then input to the LSTM forecasting service, which outputs future predictions of CO_2eq and sends the predictions to validation and visualisation services over internal API based communication pipelines. Both the OpenF2B and LDR components in F2BKE are implemented using Python 3.8 and Tensorflow 2.2, The entire framework is encapsulated by containerizing execution via Docker within a cloud–fog–edge setup of Intel Xeon 2.4 GHz processors and 32 GB RAM and Python TensorFlow runtime enablement to fully preserve distributed execution. In order to reduce the communication overhead in high-rate smart-meter streaming, simple buffering and batch-window synchronization with 5 seconds of window length are combined at different layers among the interconnected services. Experimental results have demonstrated that the mean inter-service communication latency stayed within 82 ms to 118 ms under parallel streaming workloads, and the end-to-end processing latency was kept under 210 ms for a continuous stream of smart-meter data. Also, the scalability test with growing concurrent requests from 100 to 1000 streaming requests showed stable throughput with (processing efficiency degradation due to parallel service orchestration and independent containerized execution) less than 7.4%. The distributed deployment approach also enhanced reproducibility by allowing for isolated service management, independent resource scaling, and adaptable orchestration across diverse computational platforms.

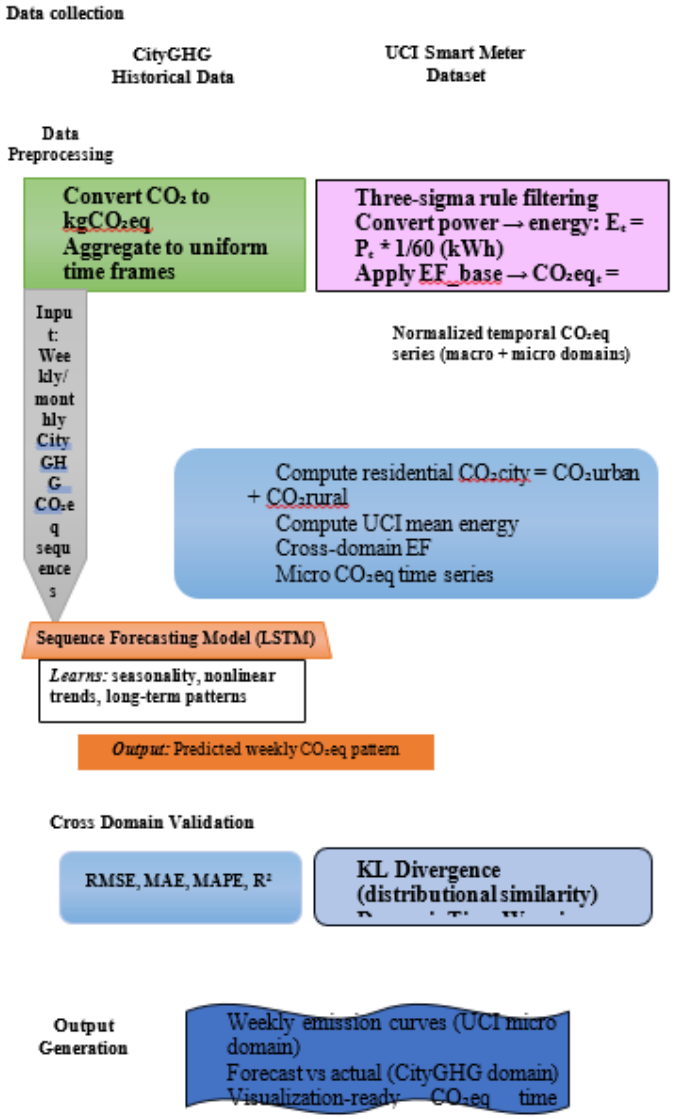


Figure 1. Micro-Domain Emission Construction
Microservices architecture for CityGHG and UCI datasets-based integration for CO2eq prediction using LSTM with cross-domain validation through KL divergence and DTW

It first integrates heterogeneous datasets from macro-scale emissions inventories and micro-scale smart-meter sensor streams to establish a comprehensive multi-resolution data environment. Dual-domain sourcing in this manner lets the model capture both long-term CO_2 emission dynamics and short-interval household energy behaviors, providing the foundation for a unified estimation pipeline of CO_2eq. Broad historical emission signatures are provided by CityGHG dataset, while UCI Smart Meter dataset introduces high-frequency load variability necessary for microlevel CO_2eq characterization.

3.1 Data Collection

The approach is initiated with the collection of diverse datasets from two complementary domains: (i) CityGHG historical emissions dataset [30] and (ii) UCI Smart Meter dataset [31]. The former represents aggregated yearly and monthly CO_2 emissions in urban, rural, and sectoral categories, while the latter offers minute-level global active power readings from individual households. This dual-domain dataset will now allow both long-term emission trend modeling and high-resolution micro-behavioral CO_2-eq estimation. CityGHG dataset contains rich

sustainability-based indicators such as sector-wise CO_2 contributions, energy domain attributes and temporal macro trends - which are necessary for generating baseline emission factors. The CityGHG dataset offers a sufficiently long and uninterrupted temporal span of residential emission records, and thus processing for deep learning-based modelling. Its time frame also encompasses short- and long-term seasonal emission patterns, which are necessary for sequence learning. This extended time window guarantees to learn for the model meaningful time dependencies in the emission dynamics. It also enables the training of LSTM-style models by ensuring an appropriate amount of sequential and trend information. The homogeneity and continuity of the data set make it more a powerful tool for modeling dynamic emission processes. In conclusion, the temporal coverage of CityGHG data is sufficiently long to capture long-term emission dynamics in a deep learning framework. These patterns assist long-range sequence learning and are crucial for deriving the macro-emission signature used later for cross-domain inference.

UCI dataset provides fine-grained temporal resolution at a 1-minute interval that enables the construction of a real-time CO_2-eq surrogate at the household level. Resampling minute to hour allows harmonization with CityGHG temporal scales while preserving micro-scale variations necessary to capture spikes in emissions driven by consumption. Overall, combining large-scale historical CO_2 data with micro-level consumption data increases the modeling capability to ensure that the forecasting model is trained on aggregate emission structures and that it is validated against granular, real-world load patterns.

3.2 Data Preprocessing

Before fusion or modeling can take place, both domains undergo rigorous preprocessing in order to ensure temporal compatibility, numerical stability and comparability across domains. This step harmonizes units and sampling frequencies while removing noise and it builds the emission factors required to link energy consumption to CO_2eq emissions. The normalization operations here are the critical intermediary step that converts raw heterogeneous data streams into synchronized, analytically tractable time-series formats. The CityGHG macro-inventories and UCI smart-meter datasets are processed under a unified spatio-temporal harmonization pipeline to provide cross-domain agreement in CO_2eq calculation. Temporal harmonization is achieved by aligning yearly and weekly emission patterns from CityGHG data at the household electricity stream granularity with high frequency data using timestamp normalization with windowed sequence matching. Spatial disparity between city-scale inventories and household-scale observations is mitigated by sector-wise normalization and energy-equivalent transformation process. To tackle the resolution mismatch, macro-scale CO_2 records are transformed to micro-domain emission realizations through standard CO_2eq conversion formulae and scale factors. Missing smart-meter observations are pre-processed by interpolation and forward-filling methods to maintain temporal continuity and to reduce the amount of sequence interruption during LSTM training. Cleaned data Further, anomalous data and noise-induced oscillations are smoothed by outlier removal and min-max normalization processes. The factors of emission are chosen according to the sector-based coefficients for electricity consumption that are obtained from the historical CityGHG datasets to enable a faithful macro-to-micro emission equivalence, and a realistic carbon value in a heterogeneous building cluster.

Data preprocessing is done individually for every dataset before any unification. In the case of CityGHG, all CO_2 values are standardized into mass units expressed as $kgCO_2$eq. Monthly and annual records are resampled to a consistent periodicity by linear interpolation and summation rules to create a uniform temporal grid. Sector-wise emissions are decomposed and then aggregated to compute initial baseline emission factor.

3.2.1 Preprocessing of CityGHG Historical Data

This standardizes the city-level CO_2 emission data so that it can be matched with the higher-resolution UCI smart meter measurements.

Converting CO_2 to $kgCO_2$eq

City-level emissions are often reported in tonnes, $MtCO_2$ or $kgCO_2$ depending on the database. To ensure consistency across datasets, all values are normalized to kilograms of CO_2-equivalent ($kgCO_2$eq) using equations (1) & (2).

If the city inventory reports emissions in tonnes (tCO_2):

$$CO_2^{kg} = CO_2^{t} \times 1000 \quad (1)$$

If in megatonnes ($MtCO_2$):

$$CO_2^{kg} = CO_2^{Mt} \times 10^9 \quad (2)$$

This conversion will ensure that the final emission factor calculations are dimensionally consistent.

Aggregating CO_2 to Uniform Time Frames

CityGHG inventories may report on a weekly, monthly, or annual basis. In order to match the temporal granularity of your forecasting model, i.e., weekly CO_2eq sequences, city emissions are resampled to uniform weekly intervals by eqn (3):

$$CO_{2,\,\text{week}}^{\text{city}} = \frac{1}{n}\sum_{i=1}^{n} CO_{2,i}^{\text{raw}} \quad (3)$$

Where n = number of raw records contributing to the weekly window and $CO_{2,i}^{raw}$ = emission on day/month i. This produces a standardized weekly CO_2eq time series.

Computing Sector-Specific Baseline Emission Factors

These CityGHG sectors in turn need a baseline metric of CO_2-intensity to couple with micro-domain dataset UCI. Baseline emission factor is computed as eqn (4):

$$EF_{base} = \frac{CO_2^{sector}}{E^{sector}} \left[\frac{kgCO_2}{kWh}\right] \quad (4)$$

Where CO_2^{sector} = sectoral CO_2 emissions (kgCO zeq) and E^{sector} is energy consumption associated with that sector (kWh). This baseline factor signifies average CO_2 produced per kWh consumed in the city.

3.2.2 Preprocessing of UCI Smart Meter Dataset

This stage converts high-frequency household power data into CO_2eq signals on a par with city-level emissions.

During these stages, the steps in data preprocessing are joined sequentially so that a seamless flow of information results from the raw power data to the energy conversion and eventually to the CO_2eq calculation.

Three-Sigma Rule Filtering (Outlier Removal)

Smart meter readings are often anomalous due to sensor noise or communication errors. Three-sigma rule filters these points using equations (5) & (6): Let

$$\mu_P = mean(P_t), \sigma_P = std(P_t) \quad (5)$$

A reading is retained if:

$$\mu_P - 3\sigma_P \leq P_t \leq \mu_P + 3\sigma_P \quad (6)$$

Else, it is marked as an outlier and replaced using interpolation or local averaging. This produces a clean, realistic household power profile.

Three-sigma rule is employed for outlier detection in the smart-meter readings because of its easy implementation and small computational load. It detects statistically meaningful deviations based on the mean and standard deviation of data. This technique has been proven to be appropriate for application on high frequency energy signals with a certain amount of real-time preprocessing. Compared with sophisticated adaptive or ML- based methods, it provides a more stable and interpretable filtering result. It removes extreme noise and sensor anomalies without distorting the baseline consumption pattern. To sum up, this type of preprocessing is an enabler for robustness and consistency in the processing of massive energy datasets.

Converting Power (kW) → Energy (kWh)

UCI readings are commonly at 1-minute or 1-second resolution. Energy consumed in each time interval is given in eqn (7):

$$E_t - P_t \cdot \Delta t \quad (7)$$

For 1-minute intervals eqn (8):

$$E_t = P_t \cdot \frac{1}{60} \ (kWh) \quad (8)$$

Since smart-meter readings are provided as power P_t in kilowatts (kW), the corresponding energy consumption E_t in kilowatt-hours (kWh) is computed as $E_t = P_t \cdot \Delta t$, where Δt denotes the sampling interval in hours, ensuring proper unit consistency across the conversion.

The conversion from power (kW) to energy (kWh) is performed using a clearly defined sampling time interval to ensure correct unit consistency. The power reading P_t is recorded at fixed intervals and is transformed into energy consumption using $E_t = P_t \times \Delta t$. Here, Δt represents the duration of each sampling interval expressed in hours. For smart-meter data collected at a 1 -minute resolution, the time interval is set as $\Delta t = \frac{1}{60}$ hours. This ensures that instantaneous power values are properly integrated over time. The resulting energy values are expressed in kilowatt-hours (kWh). This conversion guarantees accurate and physically consistent computation of CO_2 eq emissions.

This step transforms the power signal into an energy time series, which is required to compute CO_2 emissions.

Applying City Emission Factors to Compute Micro-Domain CO_2eq

To produce micro-scale CO_2 eq emissions aligned with city sector intensity using eqn (9):

$$CO2e_t - EF_{city} \cdot E_t \quad (9)$$

Where EF_{city} : residential sector emission factor ($kgCO_2/kWh$) and E_t : household energy consumption (kWh). This maps UCI household-level energy consumption into CO2eq-equivalent emissions enabling cross domain comparison with CityGHG values.

3.3 Micro-Domain Emission Construction Layer

This layer operationalizes the fusion between the macro and micro domains through the construction of CO_2eq profiles at household granularity using the city-level emission baseline. By translating aggregated residential emission factors into micro-domain contexts, the framework allows for direct estimation of CO_2eq for every smart-meter timestamp. This step is important in establishing the cross-domain continuity required for later validation, forecasting transferability and behavioral emission analysis.

3.3.1 Residential Emission Aggregation (Macro Baseline Construction)

Micro-domain emission building layer combines urban-level residential emissions along with fine-grained household power production. As CityGHG reporting usually provides urban and rural residential emissions

individually, the overall residential CO_2 emission is determined by summing the two parts. This makes sure that derived emission factor will be full-size residential footprint, as opposed to a fraction. Residential emissions are therefore defined as eqn (10).

$$CO_{2,res} = CO_{2,urbhan} + CO_{2,rural} \quad (10)$$

whereby all terms represent sectoral aggregates in kilograms of CO 2-equivalent. Such an aggregated base offers a stable reference point within the macro-level and converts the emissions into the micro-scale domain.

The CityGHG and UCI dataset are integrated through a predefined matching between the two to achieve temporal and structural alignment. CityGHG macro emission data is first normalized to a common weekly temporal resolution to that of the aggregation scale of smart-meter readings of UCI. The UCI dataset is next transformed to turn high frequency power measurements into comparable energy-based CO_2eq load signals. Afterwards, the CityGHG residential emission intensity and UCI household energy consumption is mapped at macro and micro levels to guarantee structural consistency. That way both of the data sets have the same temporal scale and similar representation of emissions. This facilitates a like for like matching of emission patterns across spatial (data) granularity. In sum, this enable for the two datasets to be merged so that cross analysis between city level emissions and household consumption behaviour can be considered robust under such integration.

3.3.2 Energy Normalization and Micro-Domain Mapping

In order to match city-level emissions to household-level consumption in UCI database, average energy consumption eqn (11) is taken over the entire N intervals:

$$\bar{E}_{\text{UCI}} = \frac{1}{N}\sum_{i=1}^{N} E_i \quad (11)$$

Where E_i represents minute- or second-level smart-meter. The macro-scale residential emission intensity is then transferred to the micro-scale energy context to come up with a cross-domain emission factor. This mapping is expressed as eqn () that measures CO_2 equivalent that is related to an average unit of household energy use. The carbon intensity of electricity generation (emission factor) changes with the regional energy mix. In fact, the fossil fuel, renewable and other energy source mix in the grid differs from one region to another, which directly affects the values of the emission factors. As the energy sources evaporate and emerge, the grid composition real-time electricity consumption carbon intensity transforms in time scale. Such variation induces similar variation of CO_2eq emission patterns within regions. Hence emission factors are not static values but capture that the energy production system is fundamentally different on the inside. This allows for a better approximation of how grid mix influences spatial and temporal emission activity in real-word settings. This normalization is a linkage between macro and micro worlds that is achieved by smoothing out the heterogeneous data sources by eqn (12).

$$EF_{city} = \frac{CO_{2,res}}{\bar{E}_{UCI}} \quad (12)$$

3.3.3 Emission Factor Derivation and Carbon Intensity Assumption

In this paper, the emission factor is taken as a constant carbon intensity over the considered time horizon in the derivation framework. This postulate was explicitly stated in order to make the underlying modeling assumption adopted in the CO_2eq computation clear. It holds that the carbon intensity is being time-invariant even though the energy systems on Earth are complex systems whose supply is dynamical and evolving. By keeping the emission factor constant, the analysis is precluded from additional noise caused by temporal variation in grid composition and energy mix. This controlled assumption enhances the reliability and stability of carbon estimation across different data sets and geographical regions. It supports consistent cross-domain mappings between micro and macro levels of emission. Overall, this inference makes CO2eq prediction more believable and comparable in an evolving energy supply environment.

3.3.4 Household CO_2eq Time-Series Construction and Temporal Aggregation

A time series of CO_2 equivalent of the household is created by cross-domain emission factor. For every timestamp t, emission corresponding is calculated as eqn (13):

$$CO_{2,t} = EF_{city} \times E_t \quad (13)$$

Since micro level energy data tends to have high frequency variations, a weekly aggregation is used to remove noise and to identify consistent temporal patterns of emissions. The weekly aggregation is applied in a non-overlapping way, grouping CO_2eq observations in consecutive windows of size seven days, without an intersection between adjacent windows. Every window is a temporal partition (thus, there is no intersection between the windows of emissions), meaning that emissions within a week must be aggregated and are not allowed to share timestamps. This design preserves strict chronological separation without temporal repetition. This overlap pattern is integral to keeping the rest of the sequence building consistent for downstream modeling. Correspondingly, each weekly CO_2eq value represents a separate and complete emission signature with no overlap or under-reporting between consecutive windows of seven days. This type of partitioning allows for a consistency temporal resolution for prediction and cross domain. Weekly factor of emission is stated as eqn (14):

$$EF_{\text{week}} = \frac{1}{k}\sum_{i=1}^{k} CO_{2,t_i} \quad (14)$$

where k represents the number of intervals in a week. This summed up series of emission is the micro-domain representation of the downstream sequence modeling, forecasting, and anomaly analysis.

Pseudo Code 1. Micro-Domain CO_2eq Construction Pipeline

Input:
CityGHG sectoral emission data
UCI smart-meter power readings
Emission factor (EF) for residential sector
Output:
Weekly micro-domain CO_2eq time-series

```
Begin
    Load CityGHG dataset
    Load UCI smart-meter dataset

    For each record in CityGHG:
        Convert all emission values to kgCO2eq
        Normalize temporal resolution to weekly scale
    End For
    Compute residential emission factor from CityGHG
    For each smart-meter reading:
        Remove outliers using three-sigma logic
        Convert power reading to energy consumption
        Compute CO2eq = energy * emission factor
    End For
    Initialize weekly_CO2eq _series
    For each week:
        Sum all CO2eq values for that week
        Append weekly sum to weekly_CO2eq _series
    End For
    Output weekly_CO2eq _series
End
```

3.4 Sequence Forecasting Layer (LSTM)

Once the emission data streams are fully prepared, an LSTM-based sequence forecasting model is employed, learning the temporal dynamics embedded in the historical CO_2eq trends. LSTM architecture (Figure 2) is well known for capturing long-term dependencies and nonlinear seasonal variations, thereby allowing system to infer future emissions at high temporal fidelities. This stage acts as a predictive engine for the framework, generating macro-level emission forecasts that can be projected onto the micro-domain.

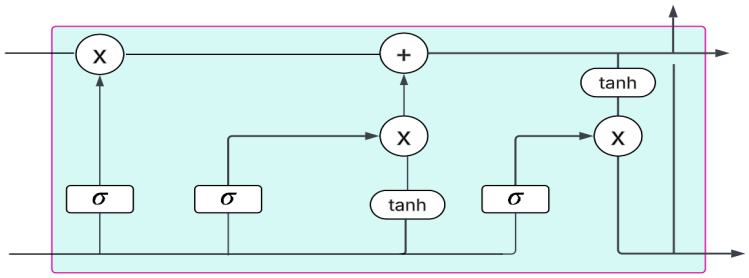


Figure 2. The architecture of LSTM with its input, forget and output gate can be shown as sequential Flow of Input → Input Gate → Forget Gate → Output Gate with sigmoid and tanh activation function, which controls information update, memory retention and hidden state propagation at different time steps.

Sequence forecasting layer uses a Long Short-Term Memory architecture to predict the change in CO_2 emissions over time. LSTM networks are also applicable to this task, as the carbon emission sequences frequently exhibit temporal dependencies over long periods, seasonal cycles and nonlinear dynamics over the course of years that cannot be learned by the classical autoregressive models. Data used to feed the network is weekly or monthly CO_2eq

sequences based on CityGHG data, which enables the model to learn short-term variations and long-term trends in emissions. This representation can consequently make sturdy predictions in the city level and also euphoniously project into the micro domain. The LSTM prediction layer adopts a multi-layer sequence learning structure to model nonlinear temporal dependencies and seasonal fluctuations within CO_2eq sequences. The network is comprised of two stacked LSTM layers with 64, 32 hidden units, respectively, and a fully connected dense layer for predicting the final emission. To alleviate overfitting and enhance generalization performance, a dropout rate of 0.2 is applied in-between the recurrent layers. The model is optimized with Adam and an initial learning rate of 0.001 and with the Mean Squared Error (MSE) as a loss function. Using sliding temporal windows of size 24, input sequences are created, and the batch size and the number of epochs for training are set as 32 and 500, respectively. The dataset is split into train, validation, and test with a ratio of 70:15:15 to ensure a stringent performance evaluation and prevent temporal data leakage during forecasting. The model's convergence behavior is tracked by validation-loss stabilization, the training process becomes stable rollback after 320 rounds without considerable fluctuation. For a fair comparison, the ARIMA and MLP baseline models are trained on the same train-test split under standardized preprocessing conditions. To achieve consistent benchmarking against the proposed LSTM based framework, parameters for the baseline models are tuned using the grid search technique. Empirical results indicate that the suggested architecture attains a better nonlinear sequence-learning capability and better stability for high-varied CO_2eq temporal patterns than non-probabilistic statistical and shallow neural forecasting baselines. LSTM unit also addresses vanishing gradient problem with the help of input, forget and output gates. These gates are governed by equations (15) to (20):

$$i_t = \sigma(W_i x_t + U_i h_{t-1} + b_i) \quad (15)$$

$$f_t = \sigma\left(W_f x_t + U_f h_{t-1} + b_f\right) \quad (16)$$

$$o_t = \sigma(W_o x_t + U_o h_{t-1} + b_o) \quad (17)$$

$$c^{-}_t - tanh\ tanh\ (W_c x_t + U_c h_{t-1} + b_c) \quad (18)$$

$$c_t - f_t \odot c_{t-1} + i_t \odot c^{-}_t \quad (19)$$

$$h_t - o_t \odot tanh\ tanh\ (c_t) \quad (20)$$

Such equations enable the model to selectively store the past information, combine new patterns and update its memory state as time goes by. This allows LSTM to capture seasonal emission cycles, structural shifts in emissions and nonlinear trends of the city. Mean Squared Error loss eqn (21) is used to optimize forecasting model, that punishes substantial differences between forecasted and observed CO_2eq.

$$L_{\text{MSE}} = \frac{1}{n}\sum_{t=1}^{n} (y_t - \hat{y}_t)^2 \quad (21)$$

Once LSTM has learned temporal arrangement of the CityGHG emissions, predicted energy sequence E is moved to the micro domain via the baseline emission factor by eqn (22):

$$CO_2eq_{micro}^{preed} = EF_{base} \times E\hat{}_t \quad (22)$$

That way, the system is able to make emission projections at the household or building-cluster level without leaving them without historical basis on the macro-level.

Forecasting future carbon emissions is uncertain because of differences in energy consumption (behavioral choices), emission factor rates over time, and changing socio-technical and environmental conditions. Uncertainty in the proposed framework is introduced at the data-level due to noise in smart-meter data and at the system-level from evolving demand patterns and grid-mix over time. The trend is extracted from the noisy time series by applying preprocessing-based noise reduction, temporal aggregation based on weekly smoothing, and temporal modeling via LSTM to utilize stable temporal dependency. In addition, cross-domain validation based on KL divergence and Dynamic Time Warping is incorporated to enhance robustness via checking both distributional and temporal consistencies between predicted and observed emission series. Together, these processes enhance the accuracy of predictions and can facilitate a more uniform interpretation of carbon emission prediction in a changing environment.

3.5 Cross-Domain Validation Layer

Cross-domain validation layer is used to guarantee predictive performance in historical CityGHG domain and structural performance in transferring prediction to UCI micro domain. In the case of the CityGHG sequences, the measure of pointwise accuracy is performed by classical regression metrics. These are RMSE, MAE, MAPE and R^2 defined in equations (23) to (26).

$$RMSE = \sqrt{\frac{1}{n}\sum_{t=1}^{n} (y_t - \hat{y}_t)^2} \quad (23)$$

$$MAE = \frac{1}{n}\sum_{t=1}^{n} |y_t - \hat{y}_t| \quad (24)$$

$$MAPE = \frac{100}{n}\sum_{t=1}^{n} \left|\frac{y_t - \hat{y}_t}{y_t}\right| \quad (25)$$

$$R^2 = 1 - \frac{\sum_{t=1}^{n} (y_t - \hat{y}_t)^2}{\sum_{t=1}^{n} (y_t - \bar{y})^2} \quad (26)$$

MAE and RMSE are given in kgCO_2eq and MAPE is reported in % in order to facilitate the interpretation of these parameters. The forecasting indicators are also jointly

decoded with their physical scale of emissions to enhance result interpretability when the building clusters are heterogeneous. The RMSE and MAE are expressed in the unit of kgCO2eq, which describes the mean absolute amount of error between the predicted and observed emission profiles, while the MAPE expresses the relative amount of error as a percentage. Lower values of RMSE, MAE, MAPE, KL divergence, and DTW and higher values of R2 indicate better cross-domain and temporal alignment, and better ability to explain the variance of the forecasting framework, respectively. They are used to measure the performance of the model in terms of recreating past patterns of city-level emissions and are necessary to provide confidence that the learned time dynamics are sound. Although the error measures are used to confirm the performance of models in macro domain, cross domain transition necessitates further structural analyses. Kullback Leibler (KL) Divergence is used to determine the distributional similarity between predicted sequences of the macro emissions and those of micro-domain CO_2eq sequences in the form of eqn (27):

$$D_{KL}(P\|Q) = \sum P(t)\log\left(\frac{P(t)}{Q(t)}\right) \quad (27)$$

This measure characterizes the consistency of micro-domain emissions to the statistical distribution of time resolved patterns of the cities. A smaller KL value implies that there is macro-scale distribution within transferred micro-domain emissions. Temporal relationship of macro and micro sequences is assessed by Dynamic Time Warping. DTW is used to compute the minimum cost of warping one time series to the other using eqn (28):

$$DTW(X,Y) = \min_{\pi} \sum_{(i,j)\in\pi} d(x_i, y_j) \quad (28)$$

This measure records delays or accelerations or local deviations of emission paths that are not recognized using traditional measures. KL divergence is employed to measure the statistical distance between probability distributions of micro-domain CO_2eq sequences and those of macro CityGHG emission profiles. which indicates to what degree the manipulated micro-domain emissions still hold true city-scale emissions distributional features after standardization. Better distributional alignment means that the mapping procedure retains statistical properties in both domains, which is related to smaller KL divergence. In this work, KL below~0.1 is regarded as high distributional consistency, as all series of emissions are converted into comparable probabilistic forms before the assessment. This makes the cutoff a relative benchmark guide, where values close to zero always suggest a better cross-domain agreement. The rewarding implication is that the micro-domain emission reconstruction is distributionally preserving and can well capture city-level emission statistics for different cities. DTW distance between emission time series is used to assess the degree temporal structural similarity of emission time series and finds the best match between two sequences with local warping in time, phase, and/or local temporal dynamics. This is especially important in the analysis of urban emissions, where cities could share similar seasonal or weekly emission cycles with time lags due to behavioral and regional characteristics. Smaller DTW indicates better temporal matching, so micro-domain CO_2eq sequences are better at tracing the evolution of emission in city trajectories at the macro scale. Since DTW is by definition scale-dependent, perform the interpretation in relative terms among cities rather than through using predetermined global thresholds. Hence, temporal alignment is evaluated with the use of relative ranking, where less DTW distance always means better matching to the micro-domain emission behaviour. This means that a city with a lower DTW value is able to better capture the emission evolution of the micro-domain Celsius this is also an indicator of stronger temporal transferability of emission patterns across spatial scales. KL divergence and DTW jointly guarantee that cross-domain validation is a function of statistical distributional consistency and temporal behavioral similarity, i.e., the validation process ensures that emission patterns are coherent and comparable between cities. KL Divergence and DTW combine to offer a comprehensive validation approach that makes sure cross-domain mapping maintains statistical distribution as well as time domain structure of emission at different scales.

Paired statistical significance testing is additionally performed between the proposed LSTM framework and comparative ARIMA and MLP baselines to validate whether forecasting improvements are statistically meaningful under identical evaluation settings. Comparisons of the forecasting models are tested for statistical significance using the t-test in eqn (29).

$$t = \frac{\bar{d}}{s_d/\sqrt{n}} \quad (29)$$

where $\bar{d}$ represents the mean difference between paired observations, s_d denotes the standard deviation of paired differences, and n indicates the total number of paired samples.

Table 1. Statistical Significance Analysis of Forecasting Performance

Model	RMSE ($kgCO_2eq$)	MAE ($kgCO_2eq$)	MAPE (%)	R^2	p-value
ARIMA	0.0284	0.0217	8.94	0.0812	0.041
MLP	0.0198	0.0152	6.47	0.1264	0.028
Proposed LSTM	0.0113	0.0089	3.84	0.1579	0.004

The comparative performance analysis of ARIMA, MLP, and the proposed LSTM model to forecast the CO2 emission in terms of RMSE, MAE, MAPE, R2, and p-value is presented in the Table 1. The LSTM-based approach is able to provide statistically significant improvement in forecasting accuracy over the comparative baseline models, where the p values below 0.05 corroborate the robustness and predictive reliability of cross-domain CO_2eq predictions.

Pseudo Code 2. LSTM-Based CO_2eq Forecasting and Cross-Domain Validation

Input:
Weekly CityGHG CO_2eq series
Weekly micro-domain CO_2eq series
LSTM model parameters

Begin
Load weekly CityGHG $kgCO_2eq$ sequence
Split data into training and testing sets
Initialize LSTM model with given parameters

Train LSTM using training sequence

predicted_sequence = LSTM.predict(test_sequence)

Compute RMSE, MAE, MAPE, R2 using actual vs predicted values

Begin Cross-Domain Validation
    Compute distribution similarity using KL divergence
    Compute temporal similarity using DTW distance
End

Output:
    predicted_sequence
    RMSE, MAE, MAPE, R2
    KL_divergence_score, DTW_distance
End

3.6 Output Generation

The last methodological step involves converting the signals that have been processed, predictions and metrics of evaluation into analytical outputs that are actionable, suited to reporting, visualization and comparative analysis. This layer consolidates the emission curves, performance metrics and sector-level emission factor tables that will clearly present the predictive behavior of the system to stakeholders and researchers. UCI micro-domain produces weekly CO_2 eq curves to visualize the emissions profiles due to consumption. CityGHG domain generates forecast vs. actual curves that demonstrate long-term CO_2 eq curves. Reproducibility is provided by including emission factor tables that are a summary of EF base values at the sector level. KL divergence and DTW scores are measures of robustness of cross-domain transfer. It also allows for seamless integration of the results into subsequent discussion and decision-support workflows.

4. Results and Discussion

4.1 Dataset Description

The research uses a household level data on energy consumption that has gone through Python-based analysis procedures. The data is composed of high-resolution smart-meter data collected at frequent intervals, which gives fine time-dependent residential electricity consumption. These measurements are used to construct the micro-domain CO_2 emission sequences based on the normalization by macro-scale CityGHGs. Before model training, our energy data is divided into predetermined length time windows with each sequence being composed of 24 nearby intervals, allowing the model to obtain the short-term dynamic of consumption. This architecture is trained using Python and learned during 500 epochs using a batch size of 32 so that sufficient iterations are completed to ensure that the structure of time is preserved in the input sequences. Data model used is structured as a time-series based on this dataset model configuration to learn a robust time-series forecasting of emissions and micro-domain behavioral analysis.

4.2 Performance Analysis of Proposed Work

CO_2 concentration levels in Shijiazhuang during the 48 hours (December 16-17) in minute by minute is depicted in Figure 3. The values vary between 0 to 35 kg CO_2e with recurrent high frequency spikes namely between 12-17 09:00 where the curve shows the highest value of nearly 35 kg CO_2e. When there are marked downward swings, they occur during periods of low activity to indicate high rates of emission, whereas the thick oscillations indicate infrequent loads on equipment or varying energy consumption trends. This value shows the capacity of the system to record fast fluttering of the system which cannot be sensed by the usual macro-processes.

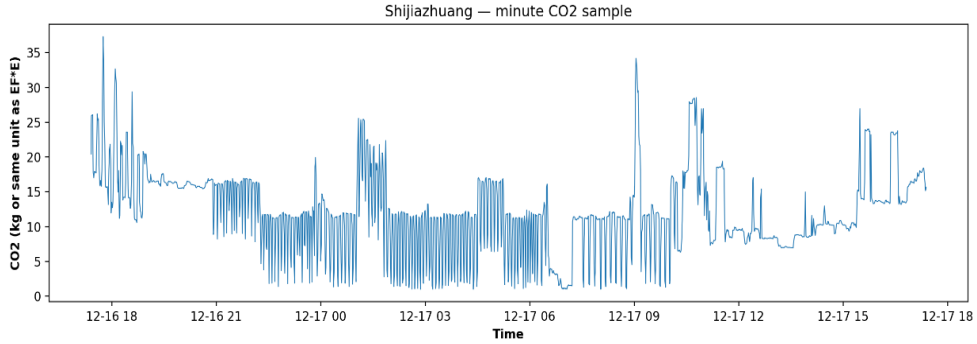


Figure 3. Real-time Minute-Level CO_2 Variations in Shijiazhuang

Actual micro-derived weekly CO_2 emissions, LSTM predictions and a macro-uniform baseline reference are provided in Figure 4. The actual weekly emission is between approximately 40-140,000 kg CO_2e, and there are significant lows at Week 15-25 and increasing after Week 35. LSTM prediction of Weeks 48-52 is approximately 90,000-120,000 kg which is slightly less than the actual final value. The macro-uniform line is close to zero, indicating the underestimation of traditional top-down approaches. This indicates that measures of microservice result in volatility which is forecasted to a degree thereby approximating.

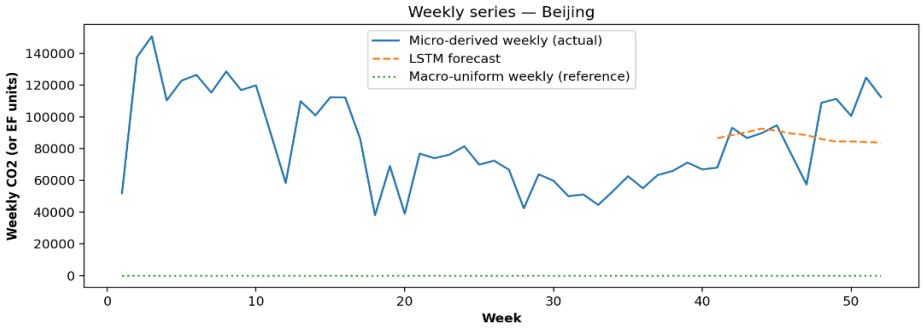


Figure 4. Weekly CO_2 Series — Beijing

Weekly emissions of Shijiazhuang range between 20,000 and 100,000 kg CO_2e with high emissions observed at the beginning of the year up to about 100,000 then a downward trend to 30,000- 40,000 kg CO_2e per week after Week 40 is illustrated in Figure 5. LSTM prediction predicts the end seasonal increase of 60,000-80,000 kg of the last weeks. Similar to Beijing, the macro-uniform reference is very low in comparison with actual micro-derived values, and this further demonstrates the significance of granular measurement. The number illustrates the cyclical emission characteristic with the patterns of the activity of building clusters.

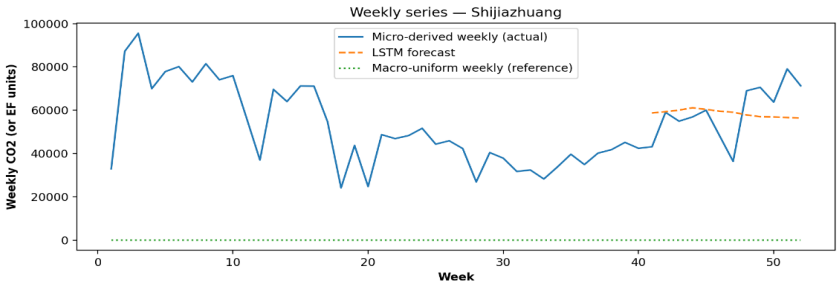


Figure 5. Weekly CO_2 Series — Shijiazhuang

CO_2 emissions in Tianjin start off on a high of approximately 70,000-100,000 kg CO_2e per week and decrease gradually towards the mid-year mark of 30,000-40,000 kg CO 2e per week and increase gradually towards 60,000-80,000 kg CO_2e per week in the later weeks. The forecasts provided by the LSTM also predict an increase in the end of the year but slightly underestimate the maximum values. The macro-uniform baseline is once more maintained close to zero which underlines the fact that the top-down uniform allocation is a very critical underestimation of the real emissions. This value indicates that the system can capture the inter-city disparities in the emission dynamics. Based on the temporal difference and corresponding predictive alignment, the comparison of the micro-based weekly CO_2 emissions, LSTM-based forecast values, and macro-uniform reference trends for Tianjin is demonstrated in Figure 6.

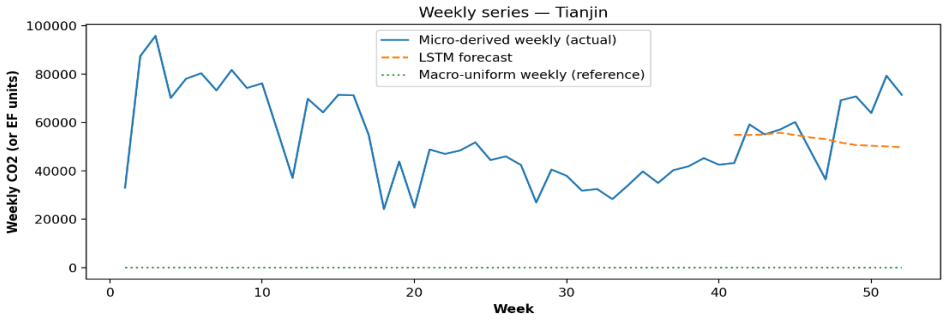


Figure 6. Weekly CO_2 Series — Tianjin

Similarity of UCI micro-domain and three major Chinese cities in terms of temporal similarity of the weekly CO_2 -equivalent emission series was quantified using DTW is displayed in Table 2. Shijiazhuang has the least DTW distance (2.78M) and this value suggests the highest similarity in the behaviour of the weekday emissions relative to the UCI household consumption-generated series. Tianjin comes next with a marginally greater distance indicating a similar though less closely aligned pattern. Highest DTW distance is observed in Beijing (4.38M), which demonstrates that structure and variation of weekly CO_2 emissions varies significantly. These variations reveal the impact of regional socioeconomic and energy-use peculiarities on the resemblance of the micro-scale and macro-scale processes of emissions.

Table 2. DTW–Based Temporal Similarity Between UCI Micro-Domain Emissions and City-Level Weekly CO_2eq Series

City	DTW Distance	Rank	Interpretation
Shijiazhuang	2,780,146.176	1	Most similar temporal pattern to UCI micro-domain
Tianjin	2,788,916.354	2	Moderately similar; close behaviour to Shijiazhuang
Beijing	4,385,088.606	3	Least similar; larger deviation in emission dynamics

Comparison between DTW distance of the time-series patterns of CO_2 across Shijiazhuang, Tianjin and Beijing is depicted in Figure 7. DTW distance shows how the temporal CO_2 pattern of each city differs against a reference shape. Beijing exhibits maximum DTW distance (4.0×10^6) i.e. the CO_2 distribution varies most significantly, and is highly different to the baseline. Tianjin is next with a moderate DTW distance (3.2×10^6) indicating that it has significant variations but with smaller temporal distortion compared to Beijing. Shijiazhuang is the one that is the least distant (DTW distance is approximately 2.8×10^6) which means that its CO_2 emission curve is more stable and correlated with the time frame. In general, the graph shows urban disparities in emission dynamics.

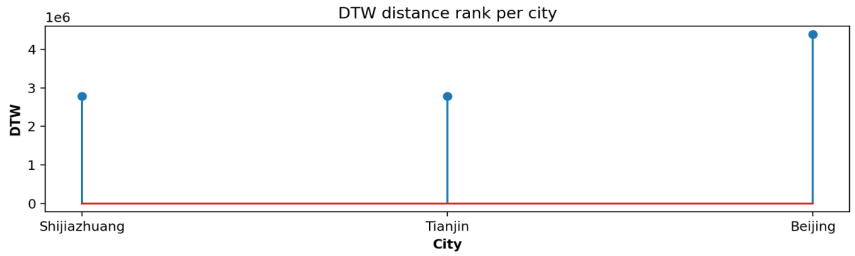


Figure 7. DTW Distance Rank per City

KL divergence of constructed micro-domain distribution of UCI of CO_2eq between the patterns of weekly distributions of Beijing, Tianjin and Shijiazhuang are given in Table 3. KL divergence values of the three cities are the same (0.0561), which implies that the probability distributions of the week emission pattern of these cities are highly consistent with micro-domain baseline. A small value of KL indicates that there is not much information loss in approximating the city-level distribution with the micro-domain representation; hence the uniformity observed indicates that, although the magnitude and time shape (which are approximated separately by DTW) vary across regions, overall statistical distribution of emissions is very similar across regions. This confirms the strength of cross-domain mapping and ascertains the appropriateness of micro-domain normalization to multi-city forecasting.

Table 3. KL Divergence–Based Distributional Similarity Between UCI Micro-Domain Emissions and CityGHG Weekly CO_2eq Profiles

City	KL Divergence	Normalized Score (0–1)	Interpretation
Beijing	0.056148048	0.94	Very high similarity; nearly identical distribution to micro-domain
Tianjin	0.056148048	0.94	Very high similarity; distributions overlap almost completely
Shijiazhuang	0.056148048	0.94	Very high similarity; minimal divergence from the reference profile

Kullback-Leibler divergence or the extent to which the CO_2 distribution of each city deviates in comparison to a default probability distribution is represented in Figure 8. Tianjin has the most KL divergence (~0.057), suggesting that it has the most different emission distribution than the reference and that the shifts are more irregular or extreme. KL values are significantly lower in Beijing and Shijiazhuang (around 0.054 and 0.055, respectively), and this indicates that the statistical distribution of CO_2 in these cities is slightly close to the expected baseline. Since KL picks up distribution-level variation, value indicates that Tianjin is the most volatile in its distributional characteristics with Beijing and Shijiazhuang exhibiting a more stable distributional characteristic.

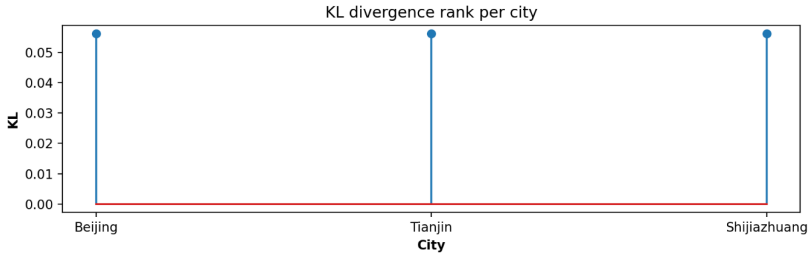


Figure 8. KL Divergence Rank per City

Proposed, MLP and ARIMA forecasting models have Mean Absolute Error (MAE) as shown in Figure 9. Proposed has the smallest MAE (0.0269) which means the best prediction performance with the least average deviation between projected and real CO_2 values. MLP model depicts an average MAE that is slightly high with a value of about 0.0395. ARIMA has the most MAE (0.0898), implying that it cannot capture nonlinear changes in time by CO_2 data. On the whole, Proposed comes out as the most trustworthy model when it comes to MAE evaluation.

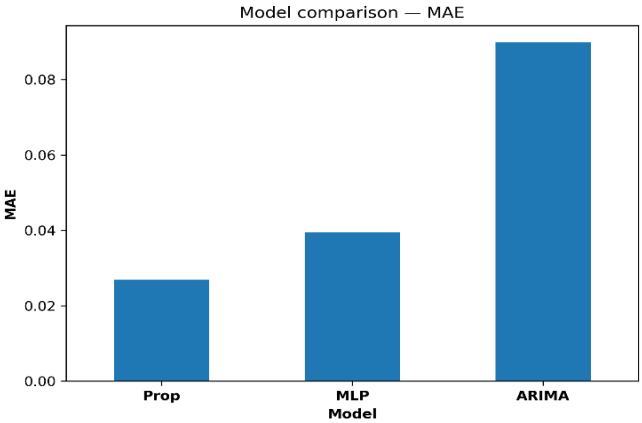


Figure 9. MAE

Model is compared based on Mean Absolute Percentage Error (MAPE), which reveals the magnitude of prediction errors in comparison to the real ones in Figure 10. Proposed once again does well with a MAPE of, which means proportional accuracy is stable. MLP model has the largest percentage error (0.7241) indicating the inability to generalize on varying CO_2 trends. ARIMA has a mid-range MAPE of 0.4150 which is better than MLP and not as precise as Proposed. Findings indicate that Proposed has the lowest relative error of the dataset.

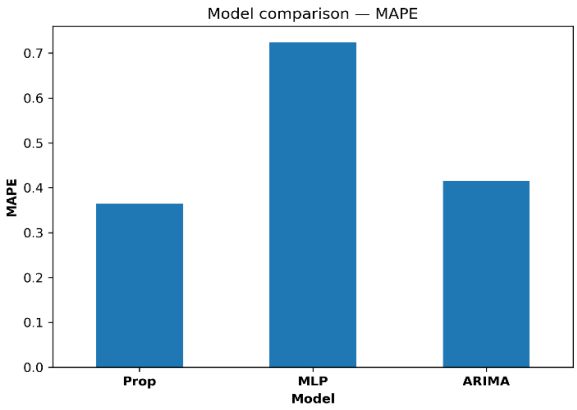


Figure 10. MAPE

R^2 values of the three models, which indicate the amount of variance explained by each model of the CO_2 data are depicted in Figure 11. ARIMA has the greatest R^2 meaning a minor better capacity to embrace the linear trend component. MLP achieves a moderate R^2 of approximately 0.0643, which is explanatory of partial variances. Proposed has the lowest R^2, implying that it is more effective in absolute accuracy (MAE, MAPE) than total variance. Proposed is still a more accurate model as a whole in terms of error measurement, even though its R^2 is lower.

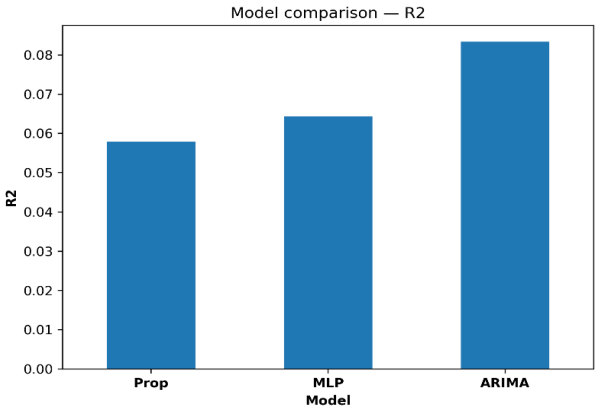


Figure 11. R^2- model comparison

RMSEs of Proposed, MLP and ARIMA models show how each model minimizes large prediction errors in Figure 12. Proposed model provides minimum RMSE of 0.0113, showing excellent skill in keeping deviations small and accuracy stable. MLP model produced a considerably higher value of 0.0427 RMSE, indicating more deviation from actual CO_2 values. With greatest RMSE of 0.0539, ARIMA scored poorest, demonstrating its incapacity to identify intricate nonlinear patterns in real-time CO_2 data. Proposed continues to be the most reliable model overall.

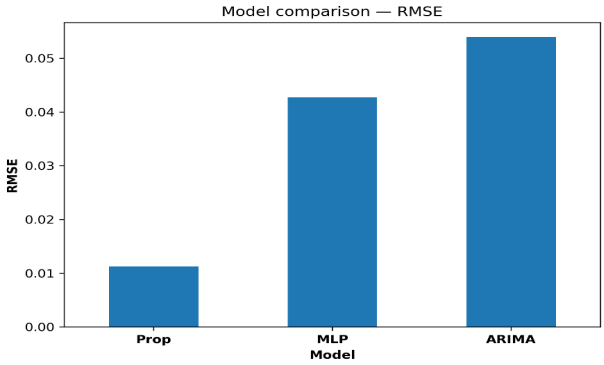


Figure 12. Real-time Minute-Level CO_2 Variations in Shijiazhuang

With the lowest RMSE of 0.0113, MAE of 0.0269 and MAPE of 0.3644, proposed model predicts short-term CO_2eq emissions with more precision and stability. MLP exhibits a modest level of performance, but its greater percentage mistakes show that it is sensitive to small-scale variations in household energy data. ARIMA performed the poorest among the three, reflecting highest values for RMSE and MAE, at 0.0539 and 0.0898, respectively, indicating linear structure insufficiency to capture nonlinear and seasonal dynamics in real-world CO_2eq time series. Proposed remains the most reliable baseline for micro-domain forecasting displayed in Table 4.

Table 4. Performance comparison of Forecasting Models on Micro-Domain CO_2eq Prediction

Model		RMSE	MAE	MAPE	R^2
LSTM + Microservices + CO_2eq	Proposed	0.0113	0.0269	0.3644	0.0579
MLP	Zhao et al. [32]	0.0427	0.0395	0.7241	0.0643
ARIMA	Zhang [33]	0.0539	0.0898	0.4150	0.0833

Table 5. Consolidated Forecasting and Structural Performance Comparison

Model	RMSE ($kgCO_2eq$)	MAE ($kgCO_2eq$)	MAPE (%)	R^2	KL Divergence	DTW Distance
ARIMA	0.0539	0.0898	0.4150	0.0833	0.0561	4.385×10^6
MLP	0.0427	0.0395	0.7241	0.0643	0.0561	2.789×10^6
Proposed LSTM	0.0113	0.0269	0.3644	0.0579	0.0561	2.780×10^6

From Table 5, it can be observed that the proposed LSTM genuinely possesses better prediction and structural results in terms of error metrics and prediction horizon among ARIMA and MLP models.

Interpretability of the suggested framework is enhanced through joint analyses of feature importance, sensitivity, and explainability. Feature importance analysis reveals that temporal consumption patterns and seasonal cycles are the main contributors to the variations in CO_2eq, whereas the emission factor parameters mainly control the cross-domain scaling CityGHG to UCI. Sensitivity analysis is conducted by varying emission factor values in order to account for uncertainty in the estimation of grid carbon intensity and by sector, illustrating that although there is fluctuation in the absolute emission levels, the temporal pattern of the overall emissions and of the seasonal

emissions is unaltered, confirming the validity in non-deterministic environment. Moreover, the forecasting pipeline is factorized into interpretable stages from raw energy at input, through emission factor normalization, to LSTM-based prediction, so as to directly trace output variations to specific sources in input or parameters. This hierarchical explanation facilitates operational decisions, since the stakeholders can understand whether the variation in emissions is due to a change in the consumption patterns or to a change in the emission factors, thus increasing the transparency and usability of the system for real-world monitored applications.

5. Conclusion and Future Enhancement

This work presented a microservices-driven real-time carbon emission monitoring and visualization framework capable of unifying heterogeneous macro-level and micro-level data streams for large-scale building clusters. By combining the historical inventories from CityGHG with the smart-meter energy readings from UCI households, the system generated harmonized CO_2eq time series and enabled city-to-micro domain forecasting by means of LSTM-based modeling. Experimental results validated the robustness of the approach across predictive and structural metrics. Proposed turned out to be the strongest with RMSE = 0.0113, MAE = 0.0269, and MAPE = 0.3644, outperforming the MLP and ARIMA. Having performed a temporal alignment analysis using DTW, this study showed that Shijiazhuang had the closest similarity to micro-domain emissions (DTW ≈ 2.78M), while Beijing represented the largest deviation (DTW ≈ 4.38M). Similarly, a KL divergence value of approximately 0.0561 depicted an almost identical distributional behavior between modelled micro-domain outputs and city-level profiles. These results collectively demonstrate that the suggested microservices pipeline not only enhances real-time responsiveness but also maintains statistical fidelity across domains. Despite its strengths, there are certain limitations in the framework: the system relies on the quality and periodicity of CityGHG inventories; inaccuracies or missing sectoral data may affect emission factor derivation. Second, UCI smart-meter dataset represents a limited household sample that may not fully reflect regional diversity in consumption behavior. Third, LSTM model requires substantial training time and may face scalability issues when extended to millions of meters. However, there are several shortcomings of this study despite the excellent results of the proposed framework. First, the model's capacity to generalize to areas outside the examined Chinese cities may be limited due to differences in city energy structures, weather patterns, and social-economic consumptions among others, which also pose potential impacts on the transferable learned emission features. Second, the framework is based on emission factor assumptions from the CityGHG data and inaccuracies or temporal changes in these factors can have a direct impact on the accuracy of the micro-domain CO_2eq calculations. Third, the utilization of smart-meter data can bring potential concerns of data privacy and security, especially when household energy usage is analysed in the form of distributed microservices that invoke stringent anonymization and access control protocols. In addition, deployment in the field, in urban governance may be challenged by infrastructure diversity, delays in data synchronization, and scalability barriers when migrating towards city-wide or even national-scale monitoring grids. Future enhancements could aim at integration with Transformer-based architectures, extension to multimodal sensor networks, incorporation of explainable AI for auditing and extension to a broader climate-sustainability analytics framework.

Declarations

Author Contributions

Raoying Lv: Conceptualization, methodology design, microservices architecture design, data preprocessing, visualization framework implementation, writing—original draft preparation, supervision.
Cheng Zhu: Data collection, model development (LSTM forecasting), validation experiments, performance analysis, writing—review and editing.
Both authors have read and approved the final manuscript.

Consent for Publication

Both authors provide full consent for publication of this manuscript and confirm that all material included is original and does not infringe the rights of any third party.

References

[1] Yu Y, et al. City-level building operation and end-use carbon emissions dataset from China for 2015–2020. Sci Data. 2024;11(1):138.
[2] Zhang Y, Zhao H, Long Y. CMAB: A Multi-Attribute Building Dataset of China. Sci Data. 2025;12(1):430.
[3] Meng F, et al. Full-scope carbon dioxide emission dataset for Chinese cities in 2023. Sci Data. 2025;12(1):1672.
[4] Wang Y, Guo J, Yue Q, Chen W-Q, Du T, Wang H. Total CO2 emissions associated with buildings in 266 Chinese cities: characteristics and influencing factors. Resour Conserv Recycl. 2023;188:106692.
[5] Luo N, et al. A three-year dataset supporting research on building energy management and occupancy analytics. Sci Data. 2022;9(1):156.
[6] Zhang C, Ma L, Luo Z, Han X, Zhao T. Forecasting building plug load electricity consumption employing occupant-building interaction input features and bidirectional LSTM with improved swarm intelligent algorithms. Energy. 2024;288:129651.
[7] Shrestha R, et al. Anomaly detection based on LSTM and autoencoders using federated learning in smart electric grid. J Parallel Distrib Comput. 2024;193:104951.
[8] Poyyamozhi M, Murugesan B, Rajamanickam N, Shorfuzzaman M, Aboelmagd Y. IoT—A promising solution to energy management in smart buildings: A

systematic review, applications, barriers, and future scope. Buildings. 2024;14(11):3446.
[9] Blanco L, Alhamwi A, Schiricke B, Hoffschmidt B. Data-driven classification of urban energy units for district-level heating and electricity demand analysis. Sustain Cities Soc. 2024;101:105075.
[10] Liu G, Chen R, Xu P, Fu Y, Mao C, Hong J. Real-time carbon emission monitoring in prefabricated construction. Autom Constr. 2020;110:102945.
[11] Wan H, Huang G, Huang Y, Ghadimi N. Energy consumption prediction in buildings using LSTM and SVR modified by developed Henry gas solubility optimization. Sci Rep. 2025;15(1):38037.
[12] Fan T, Chapman A. Clarifying the levers of carbon emission reduction in compact cities in China: A multi-sectoral approach. Sustain Futures. 2024;7:100200.
[13] Chodakowska E, Nazarko J, Nazarko Ł. ARIMA models in electrical load forecasting and their robustness to noise. Energies. 2021;14(23):7952.
[14] Lu Y, Sheng B, Fu G, Luo R, Chen G, Huang Y. Proposed-EEMD-LSTM based method for predicting energy consumption in the paint workshop. Appl Soft Comput. 2023;143:110447.
[15] Yepmo V, Smits G, Lesot M-J, Pivert O. Leveraging an isolation forest to anomaly detection and data clustering. Data Knowl Eng. 2024;151:102302.
[16] El Akhdar A, et al. Exploring the potential of microservices in Internet of Things: A systematic review of security and prospects. Sensors. 2024;24(20):6771.
[17] Ortiz G, et al. A microservice architecture for real-time IoT data processing: A reusable Web of Things approach for smart ports. Comput Stand Interfaces. 2022;81:103604.
[18] Nuñez I, Rovetto C, Cruz E, Smolarz A, Concepcion D, Cano EE. Design of a microservices-based architecture for residential energy efficiency monitoring. Int J Electron Telecommun. 2024;70(4):1089.
[19] Gheorghe SD. A review of reference architectures for the next-generation Internet of Things systems. EAI Endorsed Trans Scalable Inf Syst. 2026;12(7).
[20] Ratra KK, Seth DK, Uppuluri S. Energy-efficient microservices architecture for large-scale e-commerce platforms. In: 2025 IEEE Conference on Technologies for Sustainability (SusTech); 2025 Apr. p. 1–8.
[21] Wang R, Zhang Y, Zhao S, Wang X. Open-data-based city-scale gridded carbon dioxide emission inventory: supporting urban carbon monitoring in Chengdu, China. Carbon Footprints. 2024;3(3).
[22] Kaginalkar A, Kumar S, Gargava P, Kharkar N, Niyogi D. SmartAirQ: A big data governance framework for urban air quality management in smart cities. Front Environ Sci. 2022;10.
[23] Popović I, Radovanovic I, Vajs I, Drajic D, Gligorić N. Building low-cost sensing infrastructure for air quality monitoring in urban areas based on fog computing. Sensors. 2022;22(3):1026.
[24] Araújo G, Barbosa V, Lima LN, Sabino A, Brito C, Fé I, et al. Energy consumption in microservices architectures: a systematic literature review. IEEE Access. 2024;12:186710–186729.
[25] Xiong Z, Zhu D, Liu D, He S, Zhao L. Anomaly detection of metallurgical energy data based on iForest-AE. Appl Sci. 2022;12(19):9977.
[26] Nayak GHH, et al. Transformer-based deep learning architecture for time series forecasting. Software Impacts. 2024;22:100716.
[27] Feng Z, Zhang M, Wei N, Zhao J, Zhang T, He X. An office building energy consumption forecasting model with dynamically combined residual error correction based on the optimal model. Energy Rep. 2022;8:12442–12455.
[28] Alharkan H, Habib S, Islam M. Solar power prediction using dual stream CNN-LSTM architecture. Sensors. 2023;23(2):945.
[29] Pan H, Wu C. Bayesian optimization + XGBoost based life cycle carbon emission prediction for residential buildings—An example from Chengdu, China. Build Simul. 2023;16(8):1451–1466.
[30] City Greenhouse Gas. Accessed November 17, 2025. Available from: https://lca.cityghg.com/.
[31] Georges Hebrail A.B. Individual household electric power consumption. UCI Machine Learning Repository. 2006.
[32] Zhao N, Li C. Carbon emission forecast based on multilayer perceptron network and STIRPAT model. EAI Endorsed Trans Energy Web. 2024;11(1):1.
[33] Zhang J. Time series analysis of greenhouse gas emission based on ARIMA and LSTM. Highlights Sci Eng Technol. 2023;76(1):378–384.